

HOPF BIFURCATIONS IN THE IEEE SECOND BENCHMARK MODEL FOR SSR STUDIES

Yasar Kucukefe
ITU
Istanbul, Turkey
yasar.kucukefe@iecc.org

Adnan Kaypmaz
ITU
Istanbul, Turkey
kaypmaz@elk.itu.edu.tr

Abstract – In this paper, the first system of the IEEE second benchmark model (SBM) for subsynchronous resonance (SSR) studies is analyzed using the bifurcation theory. A nonlinear model for the SBM which consists of a synchronous generator connected to an infinite busbar through two parallel transmission lines, one of which is equipped with a series capacitor, has been developed in MATLAB. Generator damper windings are also included in the model. The existence of Hopf bifurcations in the model is verified. The stability of limit cycles (i.e. subcritical or supercritical Hopf bifurcation) is investigated by computing the first Lyapunov coefficient. The impact of the field voltage, the mechanical torque input to the generator and the infinite-bus voltage on the first Lyapunov coefficient is also explored. In the model with Automatic Voltage Regulator (AVR) and generic Power System Stabilizer (PSS), the first Lyapunov coefficient becomes negative but remains near zero indicating the existence of a generalized Hopf bifurcation. Time domain simulations verify the analytical findings.

Keywords: Hopf bifurcations, subsynchronous resonance (SSR), first Lyapunov coefficient, torsional oscillation, eigenvalues, nonlinear systems

1 INTRODUCTION

Series capacitor compensation of AC transmission systems is an effective way of increasing load carrying capacity and enhancing transient stability. However, capacitors in series with transmission lines can cause subsynchronous resonance (SSR) that can lead to turbine-generator shaft failures as occurred at the Mohave Generating Station in Southern Nevada in the USA in 1971 [1]. Since then, considerable effort has been devoted to the understanding and analysis of the SSR phenomenon by researchers and utility professionals. IEEE SSR Working Group has constructed three benchmark models for computer simulation of the SSR [2,3]. Analytical tools for studying the SSR involve frequency scanning, eigenvalue technique, time domain simulation programs [4] and the complex torque coefficient method [5].

A single-machine-infinite-busbar (SMIB) power system with series capacitor compensation is inherently nonlinear and can be modeled by sets of ordinary differential equations. The nonlinear model including the dynamics of the turbine-generator shaft system can be analyzed using the bifurcation theory. Zhu et al. [6] demonstrated the existence of Hopf bifurcation in a SMIB experiencing SSR.

Hopf bifurcation is defined as the birth of a limit cycle from equilibrium in a dynamical system governed by autonomous ODEs (Ordinary Differential Equations) under variation of one or more parameters on which the dynamic system is dependent. Supercritical Hopf bifurcations result in birth of stable limit cycles. On the contrary, unstable limit cycles are born in the case of subcritical Hopf bifurcation. Floquet theory is widely used to study the stability of limit cycles. The procedure involves the calculation of steady-state solutions, Hopf bifurcation points, the branches of periodic orbits which emanate from the Hopf bifurcation points and the computation of the *monodromy matrix* [7]. The *Floquet multipliers* are the eigenvalues of the monodromy matrix. Then by tracing the evolution of the Floquet multipliers, one can observe the stability of these solutions. One of the multipliers is always unity for an autonomous system. If all the other multipliers are inside the unit circle on the complex plane, then the limit cycle is orbitally stable.

In this paper, we employ an alternative method to investigate the stability of limit cycles. The method involves the computation of the first Lyapunov coefficient ($l_1(0)$). Positive / negative sign of $l_1(0)$ corresponds to subcritical / supercritical Hopf bifurcation. If $l_1(0)$ vanishes then the generalized Hopf bifurcation occurs.

This paper is organized as follows. Section 2 gives a brief review of the bifurcation theory. The SMIB power system under study is described and its mathematical model is obtained in Section 3. Hopf bifurcation analysis of the system is presented in Section 4. Then in Section 5, the bifurcation analysis is carried out by including the AVR and PSS in the model. The results show that the generalized Hopf bifurcation occurs in the model. Time domain simulations using MATLAB-Simulink are carried out to verify the analytical findings.

2 REVIEW OF BIFURCATION THEORY

2.1 Nonlinear Systems and Parameter Dependence

By definition, a nonlinear system is a system which does not satisfy the superposition principle. The most common way to define a continuous-time nonlinear dynamical system is to represent the system in the form of autonomous ordinary differential equations (ODEs). Consider a continuous-time nonlinear system depending on a parameter vector.

$$\dot{x} = f(x, \alpha), \quad x \in \mathbb{R}^n, \quad \alpha \in \mathbb{R}^m \quad (1)$$

where f is smooth with respect to x and α . If varying the parameter vector α results in qualitative changes in

the system dynamic behavior in a way that different behaviors (aperiodic, periodic, chaotic, etc.) and stability conditions are introduced, these changes are called *bifurcations* and the parameter vector values at which the changes occur are called *bifurcation (critical) values*.

2.2 Stability of Equilibrium Solutions

Suppose that dynamical system (1) has an equilibrium at x^0 (i.e. $f(x^0, \alpha^0) = 0$), and denote by A the Jacobian matrix of $f(x)$ evaluated at the equilibrium, $A = f_x(x^0, \alpha^0)$. If all the eigenvalues $\lambda_1, \lambda_2, \dots, \lambda_n$ of A satisfy $\text{Re}(\lambda_i) < 0$ for $i=1, 2, \dots, n$, then the system $f(x^0, \alpha^0)$ is asymptotically stable.

2.3 Bifurcation Mechanisms

There are different types of bifurcations. The most important ones are fold bifurcation, pitchfork bifurcation, transcritical bifurcation and Hopf bifurcation [8]. Fold bifurcations are associated with dynamic systems which have Jacobian matrix with a single zero eigenvalue while all the other eigenvalues remain on the left half plane. This type of bifurcation has also other names such as saddle-node bifurcation and turning point. Transcritical bifurcation is characterized by the intersection of two bifurcation curves. Pitchfork bifurcations often occur in systems with some symmetry, as a manifestation of symmetry breaking. The bifurcation corresponding to the presence of distinct pair of purely imaginary eigenvalues $\lambda_{1,2} = \pm i\omega_0$, $\omega_0 > 0$, of the Jacobian matrix $f_x(x^0, \alpha^0)$ is called a Hopf (or Andronov-Hopf) bifurcation [9].

2.4 Supercritical and Subcritical Hopf Bifurcation

Limit cycles are periodic orbits that represent regular motions in a dynamical system. Hopf bifurcations generate limit cycles from equilibrium. Supercritical Hopf bifurcation results in a stable limit cycle. On the other hand, unstable limit cycle is born in case of subcritical Hopf bifurcation. In both cases, loss of equilibrium condition occurs.

Whether a Hopf bifurcation is supercritical or subcritical can be determined by the sign of the first Lyapunov coefficient ($l_1(0)$) of the dynamical system near the equilibrium. This coefficient can be computed as follows [10]:

Suppose (x^0, α^0) is an equilibrium point of (1) where the Jacobian matrix A has a distinct pair of complex eigenvalues on the imaginary axis, $\lambda_{1,2} = \pm i\omega_0$, $\omega_0 > 0$, and these eigenvalues are the only eigenvalues of A with zero real parts. Let $q \in \mathbb{C}^n$ be a complex eigenvector corresponding to λ_1 :

$$Aq = i\omega_0 q, \quad A\bar{q} = -i\omega_0 \bar{q} \quad (2)$$

Introduce also the adjoint eigenvector $p \in \mathbb{C}^n$ having the properties:

$$A^T p = -i\omega_0 p, \quad A^T \bar{p} = i\omega_0 \bar{p} \quad (3)$$

and satisfying the normalization

$$\langle p, q \rangle = 1 \quad (4)$$

where $\langle p, q \rangle = \sum_{i=1}^n \bar{p}_i q_i$ is the standard scalar product in \mathbb{C}^n .

Then the following invariant expression gives the first Lyapunov coefficient, $l_1(0)$:

$$\frac{1}{2\omega_0} \text{Re}[\langle p, C(q, q, \bar{q}) - 2\langle p, B(q, A^{-1}B(q, \bar{q})) \rangle + \langle p, B(\bar{q}, (2i\omega_0 I_n - A)^{-1} B(q, q)) \rangle] \quad (5)$$

where B and C are symmetric *multilinear* vector functions of $x, y, z \in \mathbb{R}^n$. With a shift of coordinates in (1), $\xi = x - x^0$:

$$B_i(x, y) = \sum_{j,k=1}^n \frac{\partial^2 f_i(\xi, \alpha^0)}{\partial \xi_j \partial \xi_k} \Big|_{\xi=0} x_j y_k \quad (6)$$

$$C_i(x, y, z) = \sum_{j,k,l=1}^n \frac{\partial^3 f_i(\xi, \alpha^0)}{\partial \xi_j \partial \xi_k \partial \xi_l} \Big|_{\xi=0} x_j y_k z_l \quad (7)$$

for $i=1, 2, \dots, n$.

The software routines we have developed in MATLAB for the analytic calculation of $l_1(0)$ in the model make extensive use of the algorithms available in the continuation software MatCont [11]. Positive / negative sign of $l_1(0)$ corresponds to the occurrence of subcritical / supercritical Hopf bifurcations. If $l_1(0)$ vanishes with nonzero second Lyapunov coefficient ($l_2(0)$), then the generalized Hopf bifurcation occurs [12].

3 SMIB POWER SYSTEM MODEL

3.1 Model Description

The first system of the IEEE second benchmark model for SSR studies is analyzed. Fig.1 shows the configuration of the SMIB power system. Series capacitor compensation is applied in one of the parallel transmission lines.

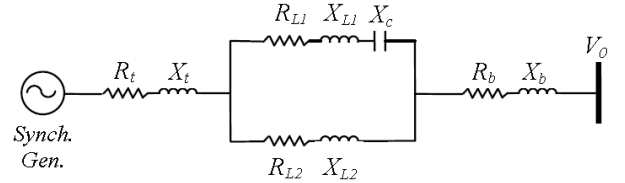


Figure 1: SMIB power system (IEEE second benchmark model for SSR studies – System-1)

The single shaft turbine generator mechanical system consists of a high-pressure (HP) turbine, a low-pressure turbine (LP), a generator and an exciter (Exc.), as shown in Fig. 2. The coefficients K and D represent stiffness and damping. Rotational inertia is represented by M . The numerical parameters are given in the Appendix.

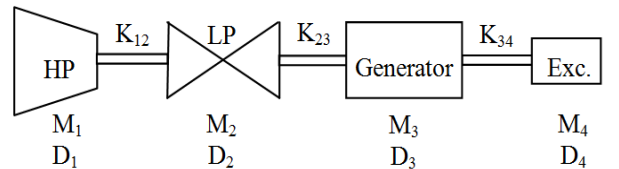


Figure 2: Schematic diagram of the mechanical system consisting of a high-pressure (HP) turbine, a low-pressure turbine (LP), a generator and an exciter (Exc.)

3.2 Mathematical Model of the System

We include the dynamics of the generator damper windings on the q- and d-axes but neglect the effect of saturation and dynamics of the turbine governor. Using

direct and quadrature (d-q) axes and Park's transformation, the complete mathematical model describing the dynamics of the electrical and mechanical systems can be written as follows [13]:

(a) *Electrical System*

Define the state variables:

$$\mathbf{i}_g = [i_d \ i_q \ i_f \ i_{kq} \ i_{kd}]^T, \quad \mathbf{i}_g \in \mathbb{R}^5$$

$$\mathbf{V}_c = [V_{cd} \ V_{cq}]^T, \quad \mathbf{V}_c \in \mathbb{R}^2$$

The equations in state space form:

$$\frac{d\mathbf{i}_g}{dt} = \mathbf{B}^{-1} \omega_b (\mathbf{C} \mathbf{i}_g + \mathbf{D}) \quad (8)$$

$$\frac{d\mathbf{V}_c}{dt} = \omega_b (\mathbf{E} \mathbf{i}_g + \mathbf{F} \mathbf{V}_c) \quad (9)$$

where:

$$\mathbf{B} = \begin{bmatrix} -(X_d + X_E) & 0 & X_{afd} & 0 & X_{akd} \\ 0 & -(X_q + X_E) & 0 & X_{akq} & 0 \\ -X_{afd} & 0 & X_{ffd} & 0 & X_{fkd} \\ 0 & -X_{akq} & 0 & X_{kkq} & 0 \\ -X_{akd} & 0 & X_{fkd} & 0 & X_{kkd} \end{bmatrix} \quad (10)$$

$$\mathbf{C} = \begin{bmatrix} (r_a + R_E) & -(X_E + \omega_r X_q) & 0 & \omega_r X_{akq} & 0 \\ (X_E + \omega_r X_d) & (r_a + R_E) & -\omega_r X_{afd} & 0 & -\omega_r X_{akd} \\ 0 & 0 & -r_{fd} & 0 & 0 \\ 0 & 0 & 0 & -r_{kq} & 0 \\ 0 & 0 & 0 & 0 & -r_{kd} \end{bmatrix} \quad (11)$$

$$\mathbf{D} = \begin{bmatrix} V_0 \sin(\delta_r) + V_{cd} \\ V_0 \cos(\delta_r) + V_{cq} \\ r_{fd} E_{fd} / X_{afd} \\ 0 \\ 0 \end{bmatrix} \quad (12)$$

$$X_E = X_t + kX_{L1} + X_b \quad (13)$$

$$R_E = R_t + kR_{L1} + R_b \quad (14)$$

$$\mu = X_c / X_{L1} \quad (15)$$

$$k = \frac{\sqrt{R_2^2 + X_{L2}^2}}{\sqrt{(R_1 + R_2)^2 + (X_{L1} + X_{L2} - \mu X_{L1})^2}} \quad (16)$$

$$\mathbf{E} = \begin{bmatrix} \mu k X_{L1} & 0 & 0 & 0 & 0 \\ 0 & \mu k X_{L1} & 0 & 0 & 0 \end{bmatrix} \quad (17)$$

$$\mathbf{F} = \begin{bmatrix} 0 & 1 \\ -1 & 0 \end{bmatrix} \quad (18)$$

(c) *Mechanical System*

Define $\mathbf{R}_s = [\omega_1 \ \theta_1 \ \omega_2 \ \theta_2 \ \omega_r \ \delta_r \ \omega_4 \ \theta_4]^T$, $\mathbf{R}_s \in \mathbb{R}^8$. In state space form:

$$\frac{d\mathbf{R}_s}{dt} = \mathbf{G} \mathbf{R}_s + \mathbf{H} \quad (19)$$

where

$$\mathbf{G} = \begin{bmatrix} \frac{-D_1}{M_1} & \frac{-K_{12}}{M_1} & 0 & \frac{K_{12}}{M_1} & 0 & 0 & 0 & 0 \\ \omega_b & 0 & 0 & 0 & 0 & 0 & 0 & 0 \\ 0 & \frac{K_{12}}{M_2} & \frac{-D_2}{M_2} & \frac{-(K_{12} + K_{23})}{M_2} & 0 & \frac{K_{23}}{M_2} & 0 & 0 \\ 0 & 0 & \omega_b & 0 & 0 & 0 & 0 & 0 \\ 0 & 0 & 0 & \frac{K_{23}}{M_3} & \frac{-D_3}{M_3} & \frac{-(K_{23} + K_{34})}{M_3} & 0 & \frac{K_{34}}{M_3} \\ 0 & 0 & 0 & 0 & \omega_b & 0 & 0 & 0 \\ 0 & 0 & 0 & 0 & 0 & \frac{K_{34}}{M_4} & \frac{-D_4}{M_4} & \frac{-K_{34}}{M_4} \\ 0 & 0 & 0 & 0 & 0 & 0 & \omega_b & 0 \end{bmatrix} \quad (20)$$

$$\mathbf{H} = \begin{bmatrix} \frac{D_1}{M_1} & -\omega_b & \frac{D_2}{M_2} & -\omega_b & \frac{(T_m - T_e + D_3)}{M_3} & -\omega_b & \frac{D_4}{M_4} & -\omega_b \end{bmatrix}^T \quad (21)$$

In (21), T_e represents the electromechanical torque and it is expressed as follows:

$$T_e = (X_q - X_d) i_d i_q + X_{afd} i_f i_q - X_{akq} i_{kq} i_d + X_{akd} i_{kd} i_q \quad (22)$$

Finally, in order to describe the complete model in state space representation form (1), we define the state vector $\mathbf{x} = [\mathbf{i}_g^T \ \mathbf{V}_c^T \ \mathbf{R}_s^T]^T$, $\mathbf{x} \in \mathbb{R}^{15}$ and combine state equations (8), (9) and (19) as:

$$\dot{\mathbf{x}} = \begin{bmatrix} \mathbf{B}^{-1} \omega_b (\mathbf{C} \mathbf{i}_g + \mathbf{D}) \\ \omega_b (\mathbf{E} \mathbf{i}_g + \mathbf{F} \mathbf{V}_c) \\ \mathbf{G} \mathbf{R}_s + \mathbf{H} \end{bmatrix} \quad (23)$$

The control parameter vector consists of the series compensation factor ($\mu = X_c / X_{L1}$), the mechanical torque (T_m), the field voltage (E_{fd}) and the network voltage level (V_0).

4 ANALYSIS OF HOPF BIFURCATIONS IN THE MODEL

4.1 Bifurcation Analysis

We use the series compensation factor ($\mu = X_c / X_{L1}$) as the bifurcation parameter and carry out bifurcation analysis. The other control parameters are kept constant ($T_m = 0.91$, $E_{fd} = 2.2$ and $V_0 = 1.0$).

Fig. 3 shows the oscillatory modes of the model. Supersynchronous and subsynchronous electrical modes have frequencies dependent on the series compensation factor. There are three torsional modes with frequencies of 24.7, 32.4 and 51.1 Hz. The local swing mode has the frequency of 1.53 Hz. In local swing mode, the turbine-generator shaft sections oscillate as a rigid body. In case the torsional modes are excited, on the other hand, some of the shaft masses oscillate against the others causing loss of fatigue life and eventually the shaft damage [14].

As μ increases, the subsynchronous electrical mode frequency decreases and interacts with all three torsional modes. The interaction results in movement of the real part of the corresponding eigenvalues towards to the zero-axis, as shown in Fig. 4.

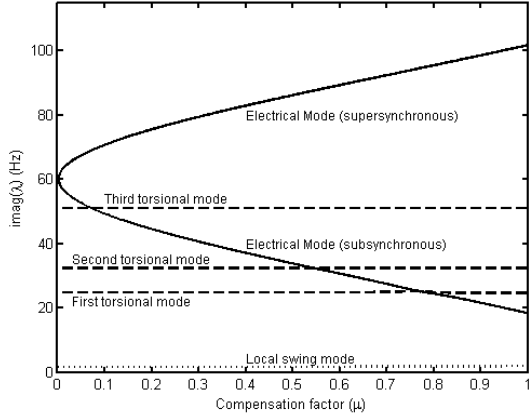


Figure 3: Oscillatory modes of the model

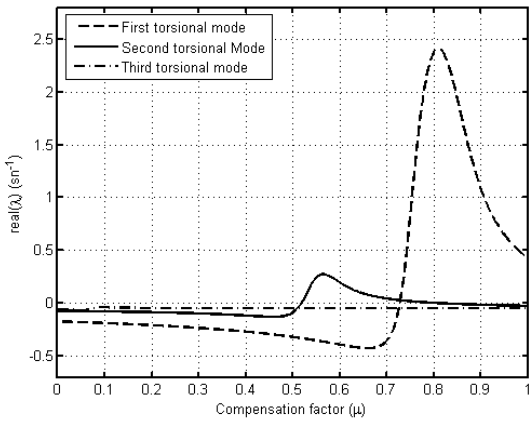


Figure 4: Real parts of the torsional mode eigenvalues

The interaction with the third torsional mode occurs at $\mu=0.07$, without causing instability. The real part of the second torsional mode eigenvalue crosses the zero-axis at $\mu=0.5184$, as a result of interaction with the subsynchronous electrical mode, and the system stability is lost through a Hopf bifurcation. Though the second torsional mode regains stability at $\mu=0.8110$, the overall system stability is not regained because of the Hopf bifurcation occurring at $\mu=0.7283$ in the first torsional mode which interacts with the subsynchronous electrical mode.

Using (5), the first Lyapunov coefficient for the Hopf bifurcation occurring at $\mu=0.5184$ is computed as 1.44×10^{-5} . From the positive sign of $l_1(0)$, we conclude that the type of Hopf bifurcation is subcritical.

Time domain simulations using MATLAB-Simulink are carried out to verify the analysis results. Fig. 5 shows the generator rotor speed response to a disturbance of 0.46 p.u. negative pulse torque on the generator shaft at $t=5$ s for a duration of 0.5s at the Hopf bifurcation point ($\mu_H=0.5184$). Following the disturbance, the generator rotor speed oscillates at decaying magnitudes until the born of limit cycles of small magnitude.

The simulation is repeated for $\mu=0.55$. Fig. 6 shows that the limit cycles do not reach to a stable orbit. It should be noted that in a real system the generator would lose synchronism following the disturbance.

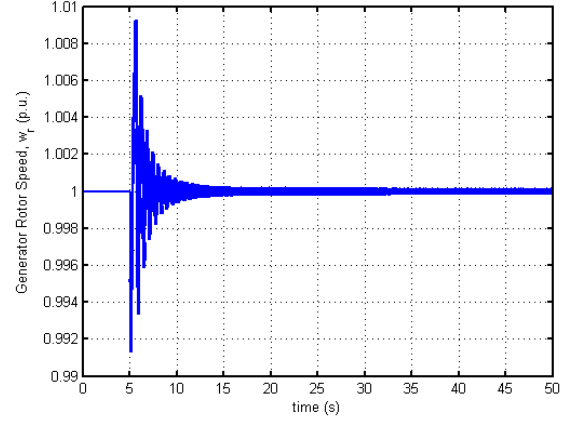


Figure 5: Generator rotor speed (ω_r) response to the disturbance at the Hopf bifurcation point ($\mu_H=0.5184$)

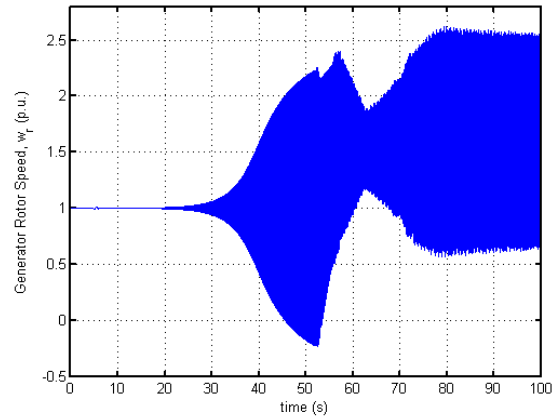


Figure 6: Generator rotor speed (ω_r) response to the disturbance at $\mu=0.55$ ($\mu_H=0.5184$)

4.2 Parameter Dependency of the Bifurcation Point and the First Lyapunov Coefficient

In addition to μ , the other control parameters T_m , V_0 and E_{fd} can affect the dynamic response of the system under study. In this section, we analyze the impact of these parameters on the Hopf bifurcation points and the first Lyapunov coefficient, thereby on the stability of limit cycles arising from the Hopf bifurcation points.

Table 1 shows the Hopf bifurcation points and the first Lyapunov coefficients for the varying values of T_m from 0.50 to 1.0 p.u. The other control parameters E_{fd} and V_0 are kept constant. It is evident from Table 1 that μ_H and $l_1(0)$ increase as T_m is raised.

T_m	Torsional Mode-1		Torsional Mode-2	
	μ_H	$l_1(0)$	μ_H	$l_1(0)$
0.50	0.6760	-0.69×10^{-5}	0.4959	0.97×10^{-5}
0.60	0.6938	-0.21×10^{-5}	0.5026	1.08×10^{-5}
0.70	0.7075	0.65×10^{-5}	0.5083	1.19×10^{-5}
0.80	0.7184	1.91×10^{-5}	0.5133	1.30×10^{-5}
0.90	0.7274	3.71×10^{-5}	0.5180	1.42×10^{-5}
1.00	0.7356	7.02×10^{-5}	0.5226	1.65×10^{-5}

Table 1: Hopf bifurcation points and the first Lyapunov coefficients at different T_m values ($E_{fd}=2.2$, $V_0=1.0$)

In Table 2, the Hopf bifurcation points and the first Lyapunov coefficients are given for the values of the field voltage (E_{fd}) from 2.2 to 2.8 p.u. T_m and V_0 are kept constant. The results show that $l_1(0)$ and μ_H of the torsional mode-1 decrease as E_{fd} is raised.

E_{fd}	Torsional Mode-1		Torsional Mode-2	
	μ_H	$l_1(0)$	μ_H	$l_1(0)$
2.0	0.7324	7.17×10^{-5}	0.5196	1.63×10^{-5}
2.2	0.7283	3.95×10^{-5}	0.5184	1.44×10^{-5}
2.4	0.7252	2.14×10^{-5}	0.5181	1.38×10^{-5}
2.6	0.7226	0.72×10^{-5}	0.5184	1.36×10^{-5}
2.8	0.7203	-0.55×10^{-5}	0.5190	1.34×10^{-5}

Table 2: Hopf bifurcation points and the first Lyapunov coefficients at different field voltages ($T_m=0.91$, $V_0=1.0$)

The bifurcation analysis results at various levels of the network voltage are shown in Table 3 for constant values of T_m and V_0 . Both μ_H and $l_1(0)$ decrease as the network voltage raises to 1.02 from 0.98 p.u.

V_0	Torsional Mode-1		Torsional Mode-2	
	μ_H	$l_1(0)$	μ_H	$l_1(0)$
0.98	0.7312	4.49×10^{-5}	0.5203	1.47×10^{-5}
0.99	0.7297	4.21×10^{-5}	0.5194	1.45×10^{-5}
1.00	0.7283	3.95×10^{-5}	0.5184	1.44×10^{-5}
1.01	0.7269	3.71×10^{-5}	0.5174	1.42×10^{-5}
1.02	0.7254	3.48×10^{-5}	0.5165	1.41×10^{-5}

Table 3: Hopf bifurcation points and the first Lyapunov coefficients for various network voltages ($E_{fd}=2.2$, $T_m=0.91$)

It is interesting to see that the impact of the control parameters T_m , E_{fd} and V_0 on the first Lyapunov coefficient is evident. Though not very significant, the changes in the computed first Lyapunov coefficients as a result of an increase or decrease in one of the control parameters exhibit a regular pattern. Hence, the accuracy of the computed first Lyapunov coefficient is found to be adequate for determining the type of Hopf bifurcation. The analysis results show that the first Lyapunov coefficients remain positive and/or near zero. Therefore, the Hopf bifurcations in the model are found not supercritical. The emphasis is given to identifying any occurrence of supercritical Hopf bifurcation condition from which stable limit cycle emanates.

5 THE MODEL WITH AVR AND PSS

Automatic Voltage Regulator (AVR) of type DC1A and power system stabilizer (PSS) described in [15] are added to the model with minor modifications. The exciter saturation effect is neglected and the limiters are omitted. Fig. 7 shows the block diagram of the excitation system with AVR and PSS. The numerical values for the AVR and the PSS parameters are provided in the Appendix.

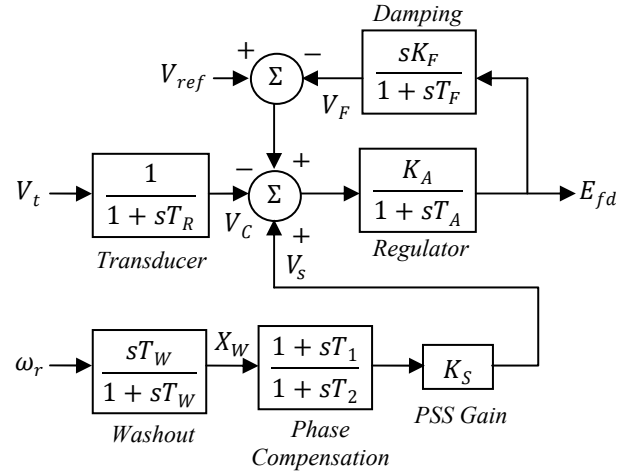


Figure 7: Block diagram of the excitation system with AVR and PSS

We include the AVR and PSS dynamics into the mathematical model (23) as follows. First define the state variables vector for the excitation system as $\mathbf{V}_{exc}=[V_C X_W V_S V_F E_{fd}]^T$, $\mathbf{V}_{exc} \in \mathbb{R}^5$. The state equation describing the dynamics of the excitation system with AVR and PSS can be written as follows:

$$\frac{d\mathbf{V}_{exc}}{dt} = \mathbf{P} \mathbf{V}_{exc} + \mathbf{Q} \quad (24)$$

where

$$\mathbf{P} = \begin{bmatrix} -\frac{1}{T_R} & 0 & 0 & 0 & 0 \\ 0 & -\frac{1}{T_W} & 0 & 0 & 0 \\ 0 & \frac{K_S}{T_2} \left(1 - \frac{T_1}{T_W}\right) & -\frac{1}{T_2} & 0 & 0 \\ 0 & 0 & 0 & -\frac{1}{T_F} & 0 \\ -\frac{K_A}{T_A} & 0 & 0 & \frac{-K_A}{T_A} & -\frac{1}{T_A} \end{bmatrix} \quad (25)$$

$$\mathbf{Q} = \left[\frac{V_t}{T_R} \quad \dot{\omega}_r \quad \left(\frac{K_S T_1}{T_2} \dot{\omega}_r\right) \quad \left(\frac{K_F}{T_F} \dot{E}_{fd}\right) \quad \left(\frac{K_A}{T_A} V_{ref}\right) \right]^T \quad (26)$$

V_t in (26) is the generator terminal voltage. Neglecting the transients, it can be expressed as:

$$V_t = \sqrt{((-r_a i_d + X_q i_q)^2 + (-r_a i_q - X_d i_d + X_{afd} i_{fd})^2)} \quad (27)$$

Combining (24) with (23), the complete mathematical model for the SMIB power system with AVR and PSS is obtained as

$$\dot{\mathbf{x}} = \begin{bmatrix} \mathbf{B}^{-1} \omega_b (\mathbf{C} \mathbf{i}_g + \mathbf{D}) \\ \omega_b (\mathbf{E} \mathbf{i}_g + \mathbf{F} \mathbf{V}_c) \\ \mathbf{G} \mathbf{R}_s + \mathbf{H} \\ \mathbf{P} \mathbf{V}_{exc} + \mathbf{Q} \end{bmatrix} \quad (28)$$

The final model has 20 state variables and these are i_d , i_q , i_f , i_{kq} , i_{kd} , V_{cd} , V_{cq} , ω_1 , θ_1 , ω_2 , θ_2 , ω_r , δ_r , ω_4 , θ_4 , V_C , X_W , V_S , V_F and E_{fd} . The control parameter vector

consists of the AVR gain (K_A), the PSS gain (K_S), the reference voltage (V_{ref}), the series compensation factor (μ), the mechanical torque input (T_m) and the network voltage level (V_0).

5.1 Bifurcation Analysis

With $T_m=0.91$, $V_{ref}=1.0982$ and $V_0=1.0$, the same operating conditions as in section 4.1, the bifurcation analysis is carried out. Fig. 8 and Fig. 9 show the oscillatory modes and the real parts of the torsional mode eigenvalues of the model with AVR and PSS, respectively.

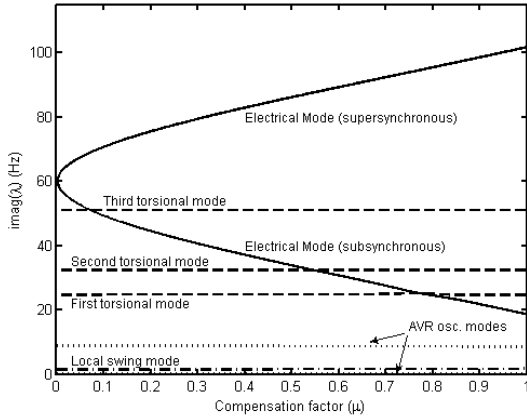


Figure 8: Oscillatory modes of the model with AVR and PSS

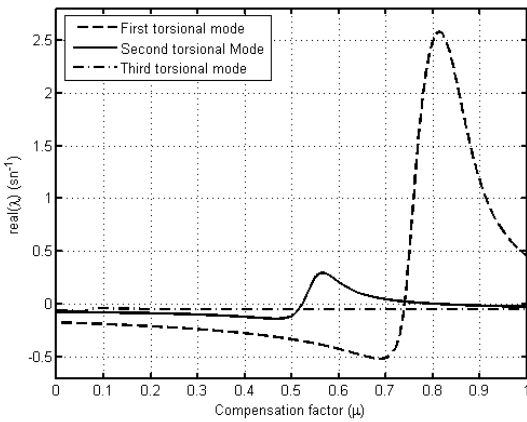


Figure 9: Real parts of the torsional mode eigenvalues of the model with AVR and PSS

Two more oscillatory modes with frequencies of 8.8 Hz and 0.22 Hz appear in the model because of the AVR and PSS. These oscillatory modes have sufficient damping and do not interact with the subsynchronous electrical mode.

Tracking the movement of the eigenvalue real parts reveals that the real part of the second torsional mode crosses the zero axis at $\mu=0.5219$. The first Lyapunov coefficient is computed as -3.59×10^{-5} . Similarly, the first torsional mode undergoes a Hopf bifurcation at $\mu=0.7403$. $l_1(0)$ value is calculated as -1.82×10^{-7} . The Bifurcation of this type in which the first Lyapunov coefficient vanishes is called the generalized Hopf bifurcation. In conclusion, the Hopf bifurcations in the model with AVR and PSS are not supercritical.

5.2 Time Domain Simulations in MATLAB-Simulink

The SMIB power system model with AVR and PSS under study is modeled using the software MATLAB-Simulink. The simulation is started in steady state with $T_m=0.91$, $V_{ref}=1.0982$ and $V_0=1.0$. The simulated disturbance is identical to the one applied in Section 4. Fig. 10 shows the generator rotor speed response to the disturbance at the Hopf bifurcation point ($\mu_H=0.5219$). Similar to the model without AVR and PSS, the limit cycles reach to a stable orbit following the initial oscillations.

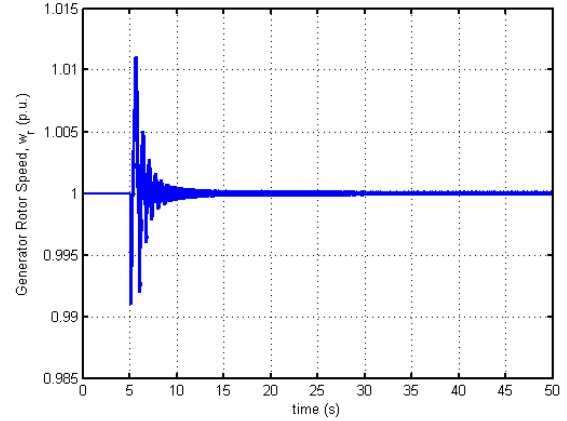


Figure 10: Generator rotor speed response to the disturbance at the Hopf point ($\mu_H=0.5219$)

With the same values of T_m , V_{ref} and V_0 , the simulation is repeated at $\mu=0.55$. Fig. 11 shows the response of the generator rotor speed to the disturbance. As a result of the generalized Hopf bifurcation, the model dynamic response bifurcates into a torus following high magnitude oscillations. This phenomenon is also called the secondary Hopf bifurcation. It is evident from Fig. 10 and Fig. 11 that the value of the series compensation factor affects dynamic response of the model to the identical disturbances.

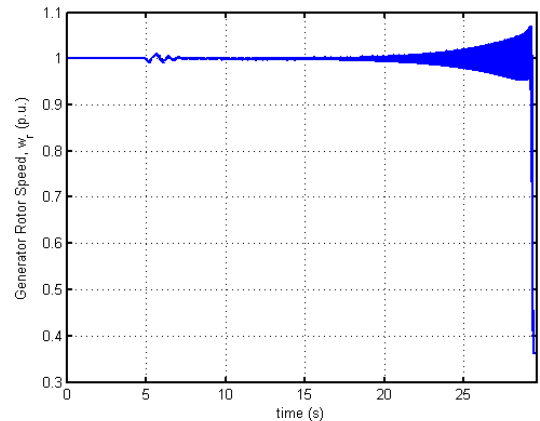


Figure 11: Generator rotor speed response to the disturbance at $\mu=0.55$ ($\mu_H=0.5219$)

In the future part of this study, control techniques for stabilizing the unstable torsional modes in power systems susceptible to the SSR will be investigated.

6 CONCLUSIONS

In this paper, we have investigated the stability of limit cycles emanating from the Hopf bifurcations in the IEEE Second Benchmark Model for SSR studies by computing the first Lyapunov coefficients. Generator damper windings are included in the nonlinear model. Taking the series compensation factor as bifurcation parameter, we have verified the existence of Hopf bifurcations in model. The first Lyapunov coefficients are computed and the results reveal that the Hopf bifurcations existing in the model are not supercritical. The impact of the mechanical torque input, the network voltage and the excitation field voltage on the bifurcation point and the first Lyapunov coefficient is also investigated.

Moreover, the AVR and PSS are included in the model and bifurcation analysis results are presented. Two new oscillatory modes appear because of the AVR and PSS. The first Lyapunov coefficients are computed and the results indicate that the generalized Hopf bifurcation occurs in the model with AVR and PSS.

The contribution we have made with this study is to use the first Lyapunov coefficient to determine the type of Hopf bifurcations existing in a SMIB power system susceptible to SSR. The applied method provides analytic results for studying the limit cycles. Time domain simulations have been carried out to verify that the method gives accurate results.

REFERENCES

- [1] IEEE Committee Report, "Reader's Guide to Subsynchronous Resonance", IEEE Trans. on Power Systems, Vol. 7, No. 1, pp. 150-157, February 1992
- [2] IEEE SSR Working Group, "First Benchmark Model for Computer Simulation of Subsynchronous Resonance", IEEE Trans. Power Apparatus and Systems, vol. 96, pp. 1565-1572, September 1977
- [3] IEEE SSR Working Group, "Second Benchmark Model for Computer Simulation of Subsynchronous Resonance", IEEE Trans. Power Apparatus and Systems, vol. 104, pp. 1057-1066, May 1985
- [4] P. M. Anderson, B. L. Agrawal and J. E. Van Ness, "Subsynchronous Resonance in Power Systems", New York, IEEE Press, ISBN 0-87942-258-0, pp. 11-14, 1990
- [5] I. M. Canay, "A novel approach to the torsional interaction and electrical damping of synchronous machine, part I: Theory", IEEE Trans. Power Apparatus and Systems, vol. PAS-101, No. 10, pp. 3630-3638, October 1982.
- [6] W. Zhu, R. R. Mohler, R. Spee, E. A. Mittelstadt and D. Maratukulam, "Hopf Bifurcations in a SMIB Power System with SSR", IEEE Proceeding of the 1995 Summer Meeting, pp. 531-534, PWRs
- [7] V. Ajjarapu and B. Lee, "Bifurcation theory and its application to nonlinear dynamical phenomena in an Electrical Power System", IEEE Transactions on

Power Systems, vol. 7, No. 1, pp. 424-431, February 1992

- [8] P. G. Drazin, "Nonlinear Systems", Cambridge, Cambridge University Press, ISBN 0-521-40489-4, pp. 6-22, 1992
- [9] R. Seydel, "Practical Bifurcation and Stability Analysis, From Equilibrium to Chaos", New York, Springer-Verlag, ISBN 0-387-94316-1, p.72, 1994.
- [10] Y. A. Kuznetsov, "Elements of Applied Bifurcation Theory", New York, Springer-Verlag, ISBN 0-387-21906-4, pp. 177-180, 2004
- [11] W. Govaerts, Yu.A. Kuznetsov, "Continuation Software in Matlab: MatCont" [Online]. Available: www.matcont.ugent.be
- [12] J. Guckenheimer, Yu. A. Kuznetsov, "Bautin bifurcation" [Online]. Available: www.scholarpedia.org/article/Bautin_bifurcation
- [13] A. M. Harb, M.S. Widyan, "Modern Nonlinear Theory As applied to SSR of the IEEE Second Benchmark Model", Bologna PowerTech 2003 Conference, Bologna-Italy, 2003
- [14] P. Kundur, "Power System Stability and Control", Electric Power Research Institute, McGraw-Hill, New York, pp. 1061-1065, ISBN 0-07-035958-X, 1994
- [15] "Recommended Practice for Excitation System Models for Power System Stability Studies", IEEE Standard 421.5-1992, August 1992

APPENDIX

The numerical parameters of the system are as follows (All units except AVR and PSS parameters in p.u. on the base of the generator ratings):

1) Synchronous generator

$$\begin{array}{ll}
 X_d=1.65 & X_q=1.59 \\
 X_{akd}=1.51 & X_{akq}=1.45 \\
 X_{kkd}=1.642 & X_{kkq}=1.5238 \\
 X_{ffd}=1.6286 & X_{afd}=1.51 & X_{fkd}=1.51 \\
 r_a=0.0045 & r_{fd}=0.00096 \\
 r_{kd}=0.016 & r_{kq}=0.0116
 \end{array}$$

2) Network

$$\begin{array}{ll}
 X_T=0.12 & R_T=0.0012 \\
 X_{L1}=0.48 & R_1=0.0444 \\
 X_{L2}=0.4434 & R_2=0.0402 \\
 X_b=0.18 & R_b=0.0084
 \end{array}$$

3) Mechanical System (Damping, Inertia and Stiffness constants)

$$\begin{array}{lll}
 D_1=0.0498 & M_1=0.498 & K_{12}=42.6572 \\
 D_2=0.031 & M_2=3.1004 & K_{23}=83.3823 \\
 D_3=0.1758 & M_3=1.7581 & K_{34}=3.7363 \\
 D_4=0.0014 & M_4=0.0138 &
 \end{array}$$

4) AVR and PSS

$$\begin{array}{lll}
 K_F=0.001 & T_F=0.1 & K_A=187 \\
 T_R=0.020 & T_A=0.001 & K_S=10 \\
 T_I=0.050 & T_Z=0.020 & T_W=10
 \end{array}$$